

MOLTEN CORE RELOCATION ANALYSIS OF CORA-17 AND CORA-18 FOR THE SAMPSON/MCRA VALIDATION

A. Prestigiacomo, A. Costa, and H. Ninokata

Dipartimento di Energia

Politecnico di Milano

via La Masa 34, 20156 Milano - Italy

andrea.prestigiacomo@mail.polimi.it; alessandro@iae.or.jp; hisashi.ninokata@polimi.it

M. Pellegrini, M. Naitoh

The Institute of Applied Energy

Shimbashi SY Bldg. 1-14-2 Nishi-Shimbashi, Minato-ku, Tokyo - Japan

mpellegrini@iae.or.jp; mnaito@iae.or.jp

ABSTRACT

Severe core damage accident analysis of Boiling Water Reactor (BWR) has gained more importance after the Fukushima-Daiichi nuclear accident in March 2011. The accident progression phenomena are governed by those mechanisms including chemical, metallurgical as well as thermal hydraulics interactions among the core materials. An exothermal reaction, i.e., high temperature Zirconium-steam interaction could lead to a temperature excursion affecting the melting progress by a positive feedback. Moreover the geometry of a BWR core complicates the modeling. The existence of channel boxes and control blades represents a significant challenge for heat transfer calculations, in particular with the thermal radiation that could not be neglected. In this paper the CORA-17 and CORA-18 experiments carried out at KfK have been selected as validation basis for the information on the damage progression of a BWR fuel element. Simulations of those experiments have been performed with the severe accident analysis code SYSTEM SAMPSON/MCRA where the models required for simulating those tests have been implemented. In the experiments the Zirconium oxidation assumes to be more important as the temperature gets higher than 1300 K, leading to a considerable heat release and hydrogen generation. Moreover a quenching phase followed the heaters shut down in the CORA-17 experiment, resulting in a much more hydrogen generation. Calculated temperature transient, rate of hydrogen generated and effects of oxidation for both CORA-17 and CORA-18 will be compared with the corresponding experimental results.

KEYWORDS

Severe accident, Molten Core Relocation, BWR, SAMPSON, validation.

1. INTRODUCTION

During the progress of severe nuclear accident, one of the most dangerous circumstances that could occur is the core melting event. Many phenomena can affect the accident progression. Among them, the most critical is represented by exothermal chemical reactions such as Zircaloy oxidation through steam interaction, resulting in hydrogen generation. This accidental condition in Boiling Water Reactors (BWRs) is more dangerous compared to Pressurized Water Reactors (PWRs) because of a larger Zr inventory within the core (e.g. the presence of channel boxes). In addition, the presence of boron carbide

(B₄C) as a neutron absorber material in control rods increases the complexity of the phenomena involved. In particular the interactions B₄C-Stainless Steel (SS) and B₄C-Zircaloy complicate the core meltdown progression (i.e. the formation of eutectic-like compounds with lower melting temperature), leading to a rapid liquefaction of stainless steel and Zircaloy well below their melting points, as pointed out by Hofmann [1] and Steinbrück [2]. Thus the presence of boron carbide could significantly affect the early phase of a severe accident. For all these reasons and for the higher geometric complexity of BWRs, it turns out that the simulation of BWRs cores with severe accident codes like SAMPSON/MCRA represents a thought issue.

The SAMPSON/MCRA code aims at computationally simulating the physical processes occurring during a meltdown of a BWR core. The models have been modified in order to take into account a wider range of phenomena, thus a validation of the code is required and is based on the analysis of the CORA-17 [3, 4] and CORA-18 [4, 5] experiments, which have been selected as representative of any BWR core meltdown conditions. These tests also represent a significant example of how the effects related to zirconium and B₄C interaction within the bundle could affect the melting process and the accident progression.

The validation consists of two parts. The former part aims at replicating the increase in temperature, taking into account the oxidation reaction of zirconium and the heat generated. The latter has the purpose to reproduce the meltdown such as core relocation, material oxidation and boron carbide interactions. For the CORA-17 experiment exists also a further phase in which quenching is performed on the bundle. This paper provides results of SAMPSON's competences, despite some deviation from CORA experimental data, which implies the need to refine the model.

2. CORA EXPERIMENTS

The CORA experiments (1986 - 1993) were carried out at the Kernforschungszentrum Karlsruhe (KfK) as part of the Severe Fuel Damage program with the intent of investigate the failure mechanisms of LWR (Light Water Reactor) fuel elements. The CORA experimental program included a total of 19 tests investigating the behavior of different type of reactor fuel elements: 11 tests for PWR; 6 tests for BWR; 2 tests for VVER (Vodo-Vodyanoi Energetichesky Reaktor). The experiments analyzed in this paper were designed in order to take into account the geometric arrangement and materials of a typical BWR fuel bundle. In these tests, severe accidental conditions were reached by electrical heaters used to simulate the decay heat of fuel, and a steam inlet mass flow rate, used to allow the zirconium-steam exothermal reaction. The selected CORA experiments have been chosen as test for the validation and verification of the SAMPSON/MCRA severe accident analysis code because they represent dry core condition and flooding event typical of the Fukushima-Daiichi nuclear accident.

2.1. Bundles description

The bundle of the CORA tests considered were constituted by fuel rods arranged on a square lattice with a pitch of 14.3 mm. The rod outer diameter was 10.75 mm, thus the pitch-to-diameter ratio assumes typical BWR values (i.e. P/D = 1.33). Fuel rods were of two different types: heated rods and unheated rods. Unheated rods were made of UO₂ pellets with 0.2% U-235 enrichment and 9.1 mm diameter. Heated rods, instead, were made by annular pellets of UO₂ with the same external diameter. Inside these pellets a tungsten heater of 6 mm diameter was contained. The active fuel length of heated rods was 1 m long. Both rods types were displaced in a staggered arrangement and were enclosed in a Zircaloy-4 cladding of 0.725 mm thickness. These rods were displaced symmetrically to the control rods, placed at the center of the bundle. The central channel was constituted by two Zircaloy slabs that represent the channel boxes of a typical BWR bundle, and a control blade was placed in-between them. The control blade was made of steel and surrounds 11 control rods containing B₄C powder with stainless steel cladding with an outside

diameter of 5.77 mm. The bundle was surrounded by a Zircaloy shroud enclosed in a ZrO_2 insulating fiber with 20 mm thickness. Inside the shroud the rods were supported by a Zircaloy spacer grid at 578 mm from the bottom with 42 mm height. Table I points out some specifics of each test bundle, while Figure 1 shows a top view sketch of both CORA-17 and CORA-18 test bundles.

Table I. CORA-17 and CORA-18 test bundles specifics [3 - 5].

	CORA-17	CORA-18
FUEL RODS		
Heated fuel rods	12 rods	28 rods
Unheated fuel rods	6 rods	20 rods
Total fuel rods	18 rods	48 rods
CHANNEL BOX		
Material	Zircaloy-4	Zircaloy-4
Wall thickness	1.2 mm	1.2 mm
Outside dimensions	86x13 mm	138x13 mm
SHROUD		
Material	Zircaloy-4	Zircaloy-4
Wall thickness	1.2 mm	1.2 mm
Outside dimensions	68x112 mm	138x135 mm
ABSORBER BLADE		
Material	S.S.	S.S.
Wall thickness	1 mm	1 mm
Outside dimensions	68x8 mm	68x8

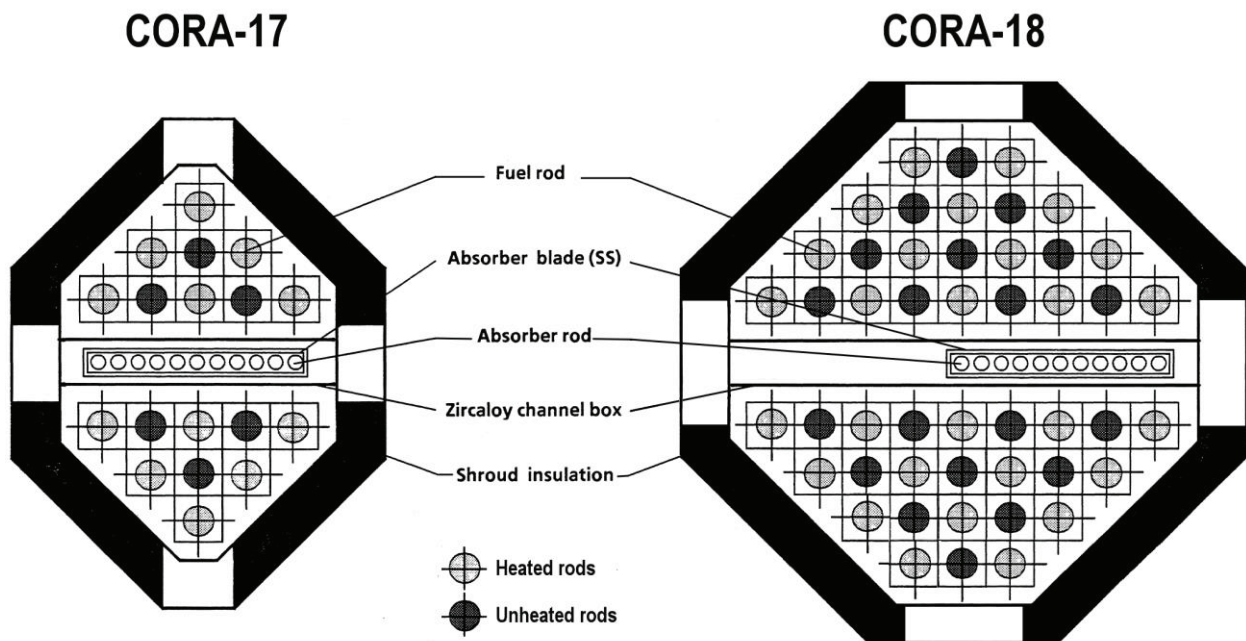


Figure 1. Top view of the CORA-17 [4] and CORA-18 [5] test bundles.

2.2. Event Sequences

The CORA tests were divided in several phases, as presented in Table II.

Table II. Phases of CORA-17 and CORA-18 experiments [4].

Phase	CORA-17	CORA-18
Gas pre-heating phase	0 - 3000 s	0 - 3000 s
Transient phase	3000 - 4820 s	3000 - 4150 s
Cool down phase	4820 - 5000 s	> 4150 s
Quenching phase	> 5000 s	--

In both tests, the bundle in the first phase was heated up with a gas injection of argon at about 500°C [4]. The argon mass flow rate was 8 g/s in the CORA-17 test while it was 16 g/s in the CORA-18 experiment. In the second phase the heaters were turned on. In CORA-17 the input power linearly grew up from 4.26 kW to 22.5 kW at 4530 s, and then it remained constant till the end of the transient phase. In CORA-18 the input power starts from 12 kW and reached the value of 39 kW after 1150 s at the end of this phase. A constant steam mass flow rate was injected from the bottom, in addition to the argon inlet, starting from 3300 s. In CORA-17 the steam inlet was 2 g/s and lasted till the end of the transient phase, while in CORA-18 the amount of steam was double and injection was stopped at 4080 s. In the third phase both tests experienced a cool down phase, in which heaters and steam inlet were turned off. The CORA-17 experiment was characterized by an additional phase in which the degraded bundle was flooded by a water injection from the bottom, with an inlet velocity of 0.01 m/s.

3. THE SAMPSON CODE

SAMPSON (Severe Accident analysis code with Mechanistic, Parallelized Simulations Oriented toward Nuclear Fields) is a severe accident code, under development at the Institute of Applied Energy, with the sponsorship of the Japanese Ministry of Economy, Trade and Industry. SAMPSON performs detailed calculations of physical and chemical phenomena in a nuclear power plant, such as fuel cladding damage, fuel melting, crust formation, molten debris cooling and fission products release. These calculations lead to an evaluation of reactor vessel and containment structural integrity.

MCRA (Molten Core Relocation Analysis) is one of the modules of SAMPSON, which simulates the relocation behavior of a molten core during severe accidents of light water reactors. The behavior of the molten core is most important for evaluating the in-vessel retention of a molten core. MCRA adopts a “multi-phase, multi-component and multi-velocity field” approach.

In the SAMPSON code, mechanistic models and theoretically based equations are maximally adopted by avoiding the use of empirical correlations as much as possible.

Typical mechanistic models are included in the MCRA module as follows:

- Multi component model
- Mass conservation equations for 9 liquid components and 6 gas components.
- Energy conservation equations for 9 liquid components and for a mixture of 6 gas components.
- Momentum conservation equations for 2 groups of liquid components (e.g. water and molten materials mixture) and one equation for a mixture of 6 gas components.
- Interaction between three phases described by an interfacial area considering phase change.

The models of both CORA experiments discussed in the present paper have been generated using the same procedure. In particular 2D models have been set up in Cartesian x-z coordinate system. The models

take into account only the part of the system enclosed within the shroud (thus shroud thermal insulator has not been modeled) and a total height of 1 m. The bundles have been divided into three main regions:

- The northern region containing: half of the shroud, half of the fuel rods (heated and unheated) and the northern channel box
- The central region containing: the control rods and the control blade
- The southern region containing: the southern channel box and the remaining half of shroud and fuel rods.

These 3D regions have been rearranged in order to obtain a total of 5 bi-dimensional channels, as pointed out in the following sub-section regarding the modeling of the CORA geometry.

3.1. Geometrical Model

The geometrical model of the CORA experiments has been obtained by dividing the domain into five channels containing a rod and a structure each. Rod lumps a greater number of real rods (heated or unheated). Since two of the regions introduced above contain two lumped rods (one for heated and one for unheated fuel rods) and two structures (half shroud and channel box), these regions should be further divided into two channels each, as a consequence. In this way channels 1 and 2, as much as channels 4 and 5, are a closed region exchanging heat by radiation and convection with the flow. The same is true also for channel 3, that corresponds to the central region without any further subdivision since it already contains a rod (representing the 11 control rods) and a structure (control blade, divided in left and right halves). These three closed region exchange heat by conduction through the two channel boxes. Each channel is axially divided into 10 equal cells. Figure 2 shows a representation of the geometrical model of the domain. In the picture *Sh* stands for shroud, *ChB* for channel box, *CoB* for control blade, *H* for heated fuel rods, *U* for unheated fuel rods and *C* for control rods. The spacers have been modeled by increasing the volume fraction and surface area of the Zircaloy structures in the sixth axial subdivision (i.e. for $k = 6$), corresponding to the elevation where the grid spacer was placed in the CORA experiments, at 578 mm from the bottom. The spacer grid has been assumed of 1 mm thickness and 50 mm height. In Figure 2, the increase in the volume fraction is graphically pointed out.

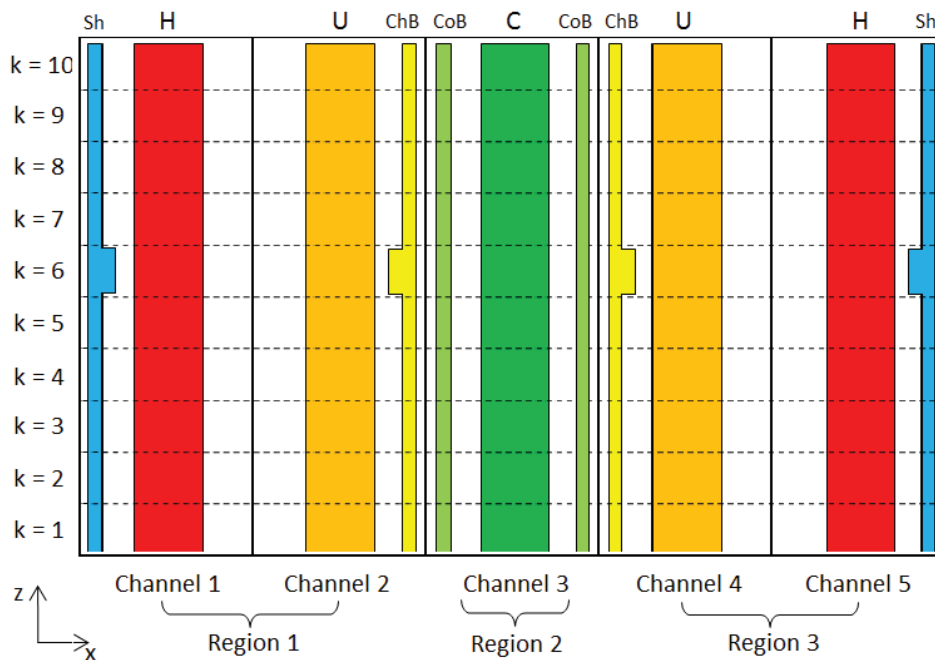


Figure 2. Sketch of the geometric model of the CORA test bundle.

3.2. Initial and Boundary Conditions

Initial temperature condition has been set to each component of the CORA domain (i.e. channels' rod and structure), accordingly with available experimental data. The chosen values are reported in Table III below for each axial cell:

Table III. Initial temperature set for CORA experiments.

Axial cell	CORA-17		CORA-18	
	Fuel rods	Structures and Control rods	Fuel rods	Structures and Control rods
k=1 (50 mm)	547.3 K	701.4 K	593.0 K	642.6 K
k=2 (150 mm)	580.7 K	675.1 K	632.8 K	642.6 K
k=3 (250 mm)	614.2 K	645.8 K	657.6 K	642.6 K
k=4 (350 mm)	647.6 K	616.5 K	661.5 K	642.6 K
k=5 (450 mm)	633.7 K	615.4 K	663.5 K	642.6 K
k=6 (550 mm)	619.7 K	614.3 K	665.5 K	642.6 K
k=7 (650 mm)	574.5 K	576.5 K	665.6 K	642.6 K
k=8 (750 mm)	529.3 K	538.7 K	652.6 K	642.6 K
k=9 (850 mm)	544.1 K	500.8 K	631.9 K	642.6 K
k=10 (950 mm)	558.9 K	463.0 K	613.1 K	642.6 K

Inlet boundary condition consisted of fixed inlet velocity and inlet gas-mixture temperature and relative molar composition. The relative molar composition has been set to 0.357 and 0.643 for steam and argon respectively. The temperature of the inlet gas-mixture has been set to 701.4 K for CORA-17 test and to 813.0 K for CORA-18 experiment. Inlet velocities have been set to 1.09 m/s and 1.00 m/s for CORA-17 and CORA-18 tests respectively. Outlet boundary conditions have been set for outlet pressure to the value of 2.2 bar for both CORA tests. As last, a heat flux boundary condition has been set on the whole shroud. In particular the flux magnitude has been imposed in order to obtain an out-coming power through the shroud surface at a fixed percentage of the input power provided by the heated rods. The selected percentages have been set to 50% and 40% for CORA-17 and CORA-18 experiment, respectively. When the shroud in a cell melts, the heat flux through the boundary is taken into account.

3.3. Physical Modeling

New physical models, that need validation, have been introduced in the SAMPSON/MCRA code. The model of the zirconium oxidation reaction, pointed out in Eq. (1), has been improved, leading to a better prediction of hydrogen generation.



The reaction rate of Eq. (1) is strongly dependent on temperature, especially above about 1300 K. Moreover this reaction is exothermal i.e. more heat is released into the system, leading to a positive feedback. The temperature dependence of the reaction rate has been implemented by considering a Arrhenius-type correlation. The best accordance has been obtained with the Prater correlation for the oxidation of α -Zr(O), as pointed out in [6]. In particular the reaction rate k is given below:

$$k = A \exp(-B / T) \quad (2)$$

In Eq. (2) the reaction rate k depends from temperature T through coefficients A and B . In the Prater correlation for α -Zr(O) the values of A and B coefficients are $12.233 \text{ kg}^2/\text{m}^4\text{s}$ and 19182 K^{-1} for $T < 1800 \text{ K}$ and $4000 \text{ kg}^2/\text{m}^4\text{s}$ and 27422 K^{-1} for $T > 1800 \text{ K}$, respectively [6, 7].

The Zr-SS and B_4C -SS interactions to form eutectic-like compounds have been taken into account by the SAMPSON/MCRA code, as pointed out in [6]. In particular the B_4C -SS interaction leads to a rapid liquefaction of both boron carbide and stainless steel at about 1500 K [8], well below the melting points of the single components. In the same way, the Zr-SS interaction leads to a lower melting point that starts at 1273 K and leads to a complete liquefaction around 1500 K [9].

In the CORA experiments the heat between channel boxes and control blade is transferred through radiation. In the model adopted these surfaces are in contact, thus the radiation exchange between the channel box and control blade surfaces should be modeled by considering a temperature-dependent conductive heat transfer coefficient that simulates the radiation exchange. Therefore, through the Fourier's Law for the conductive heat transfer and the equation of radiation exchange between two surfaces in an enclosure, the conductive heat transfer coefficient k can be expressed as follows:

$$k = \frac{\sigma L}{A_{ChB}} \left(\frac{1-\varepsilon}{\varepsilon A_{ChB}} + \frac{1}{A_{ChB} F_{ChB \rightarrow CoB}} + \frac{1-\varepsilon}{\varepsilon A_{CoB}} \right)^{-1} \left(\frac{T_{ChB}^4 - T_{CoB}^4}{T_{ChB} - T_{CoB}} \right) \quad (3)$$

In Eq. (3) T_{ChB} and T_{CoB} are respectively the temperatures of the channel box and control blade, A_{ChB} is the surface of the channel box facing the control blade, A_{CoB} is the surface of the control blade facing the channel box, σ is the Boltzmann constant and L is the thickness which, in this case, is assumed to be 1 mm . To simplify the calculation, the emissivities ε of the channel box and the control blade have been assumed as having the same value. The temperatures of the channel box and control blade are known from the experiments, therefore it is possible to calculate k using Eq. (3). From the temperature measurements in CORA-18 at 550 mm elevation it has obtained the results reported in Figure 3.

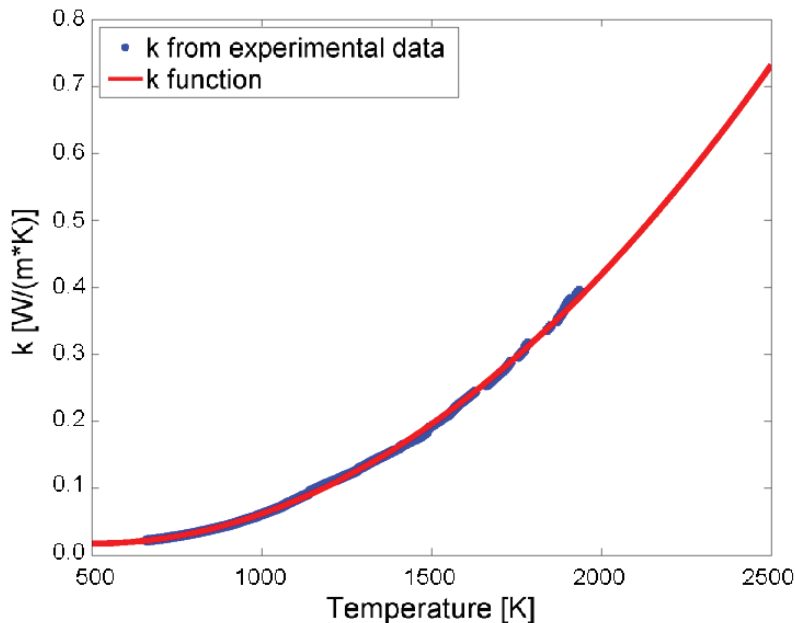


Figure 3. Conductive heat transfer coefficient calculated from experiment and best fitting function.

Using the calculated values of k , it has been possible to extrapolate a best fitting function, Eq. (4), in which k is expressed as depending on the temperature of the channel box.

$$k(T_{ChB}) = 1.79 \cdot 10^{-7} \cdot T_{ChB}^2 - 1.79 \cdot T_{ChB} + 0.06 \quad (4)$$

Equation (4) has been included in SAMPSON to calculate the conductive heat transfer coefficient between the channel box and the control blade.

4. SIMULATIONS RESULTS

In this section the main results of both CORA-17 and CORA-18 experiments simulation will be shown. In particular temperature and hydrogen production obtained will be compared with experimental data. It has been chosen to do not simulate the gas pre-heating phase (i.e. from 0 s to 3000 s) because in this phase no physically significant phenomena happen. Moreover the end of this phase can be reached by setting proper boundary conditions. Thus the simulation time shown in this section will start from 3000 s of the experiment time-line. The results shown will concern the transient and cool down phases for CORA-17 test (i.e. from 3000 s to 5000 s), and only the transient phase for CORA-18 (i.e. from 3000 s to 4150 s).

4.1. Rod and Structure Temperatures

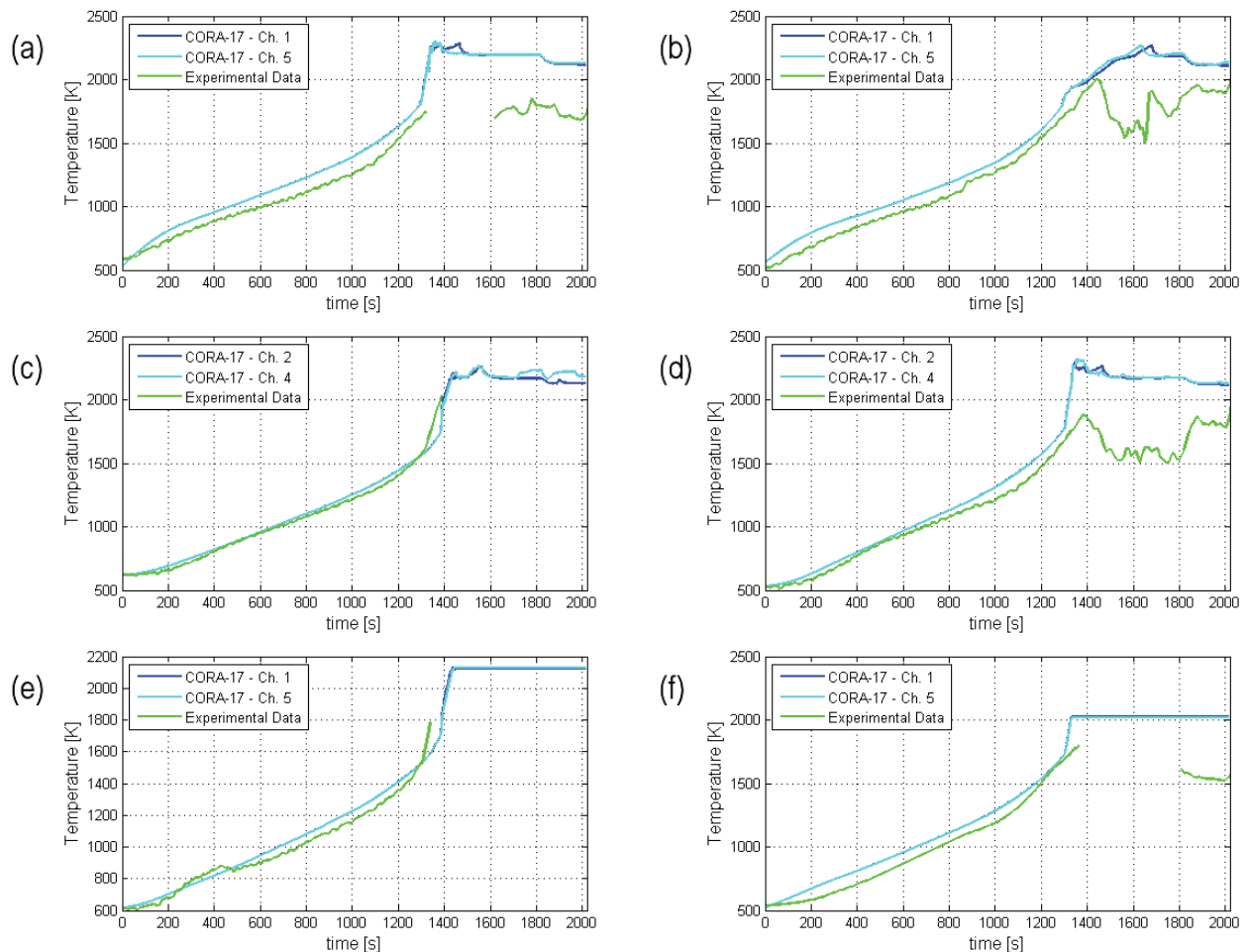


Figure 4. Temperature results for CORA-17: (a) heated rods at 750 mm, (b) heated rods at 950 mm, (c) unheated rods at 550 mm, (d) unheated rods at 750 mm, (e) channel box at 550 mm and (f) channel box at 750 mm.

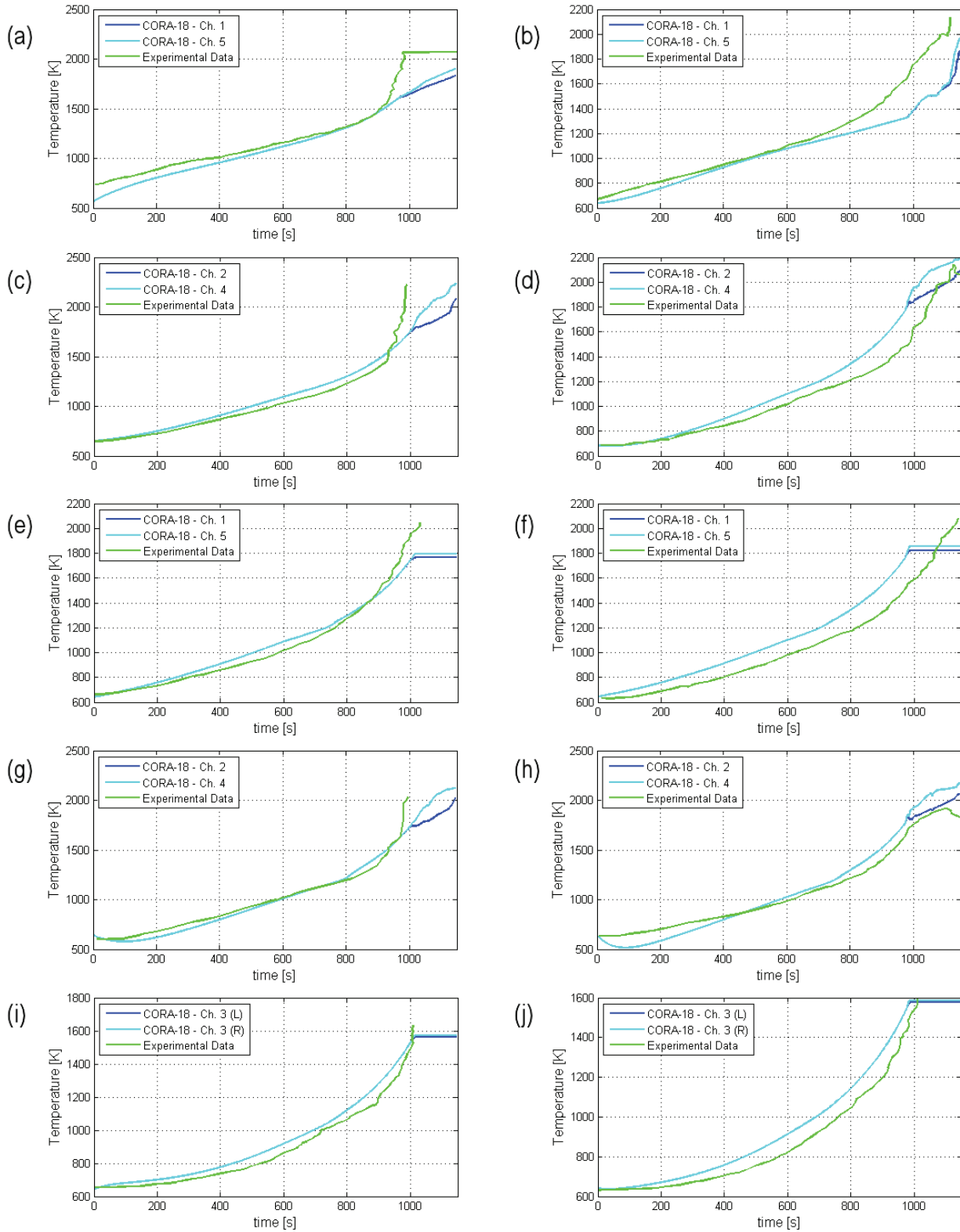


Figure 5. Temperature results for CORA-18: (a) heated rods at 550 mm, (b) heated rods at 750 mm, (c) unheated rods at 550 mm, (d) unheated rods at 750 mm, (e) channel box at 550 mm, (f) channel box at 750 mm, (g) shroud at 550 mm, (h) shroud at 750 mm, (i) control blade at 550 mm and (j) control blade at 750 mm.

The temperature results reported above shown good agreement for both CORA tests with experimental data when the hydrogen generation reaction is still negligible i.e. below 1300 K. This suggests that the energy balance within the code is fulfilled. Later on, for higher temperatures, some deviations are visible, especially in the graphs at 550 mm where grid spacers are placed. In the graphs concerning CORA-17 (Figure 4) there exist great discrepancies with experimental data after about 1300/1400 seconds. It is possible that the support of the thermocouple deforms at this time, increasing the space between the thermocouple and the rod or structure under measurement. In fact the thermocouples in CORA experiments are not welded on structures and rods. Thus the temperatures measured after that time in CORA-17 experiment could be related to the gas flow, rather than structures and rods. Nevertheless the over prediction of hydrogen generation (see section §4.2), that became important after about 1300 s in CORA-17, contributes in over predicting the temperatures of Zirconium structures and cladding. This effect exists also in CORA-18, although in this case the temperatures are mainly under predicted in the later part of the simulation.

4.2. Hydrogen Generation

The hydrogen generation rate due to Zirconium-steam interaction of both CORA-17 and CORA-18 is shown in Figure 6 in which the simulated results are compared with experimental data [5, 10]. It should be pointed out that, in both cases, computational results over predict the experiment, thus in the code more heat is provided by this reaction, as pointed out in Eq. (1), leading to an over-prediction of computed temperatures. As already mentioned in section §3.3 the higher temperatures accelerate the reaction rate, governed by Eq. (2), releasing higher power in the system. The over prediction of the hydrogen generation rate in CORA-17 (Figure 6-a) is heavier than CORA-18 (Figure 6-b), leading to a higher positive feedback.

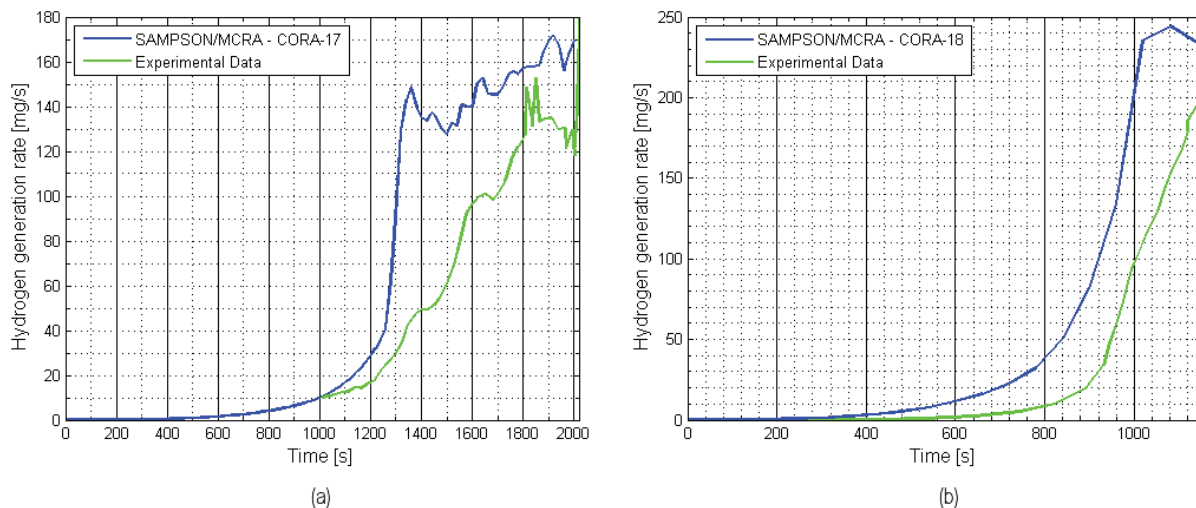


Figure 6. Results of hydrogen generation rate for CORA-17 (a) and CORA-18 (b).

4.3. Meltdown

The post-test appearance of CORA-17 bundle [4] is shown in Figure 8 for different heights, while Figure 9 shows those of CORA-18 [5]. Figure 7, instead, shows a representation of the state of the bundle for CORA-17 (Figure 7-a) and CORA-18 (Figure 7-b) at the end of the simulated transients. It is important to stress out that this representation is not related to the actual geometry of the bundle but it is related to the model described in section §3.1 with particular regard to Figure 2. By comparing the pictures shown in Figure 7 with those of Figures 8 and 9, the following considerations can be pointed out. The melting of

the control rods, control blade and channel boxes are in good agreement with post-test pictures for both experiments. The only exception regards the lowest portion of the CORA-17 bundle, as seen by comparing Figure 8-a with Figure 7-a from 0 to 100 mm of elevation. Also the presence of a portion of the control blade in the same picture (Figure 7-a) disagree with Figure 8-c. Also the condition of the shroud is in fairly good agreement with experimental data. In particular the shroud almost completely melts in CORA-17 tests (Figure 8) while in CORA-18 test it experiences a partial melting (Figure 9). In this case the major discrepancies are related to the CORA-18 results in which the shroud has disappeared only in the central region (Figure 7-b) and not at higher elevations, as it should have been. For what concerns fuel rods, instead, the code prediction is in contrast with the post-tests pictures for both CORA experiments. The presence of debris particles in the lower part of the bundle and the presence of debris crust deposited on the rods, in both CORA cases, are in accordance with the relocated material shown in Figures 8 and 9. Nevertheless the sketches of Figure 7 constitute a representation of a bi-dimensional model, thus the information regarding debris particles should be considered only qualitatively and not quantitatively.

Before moving to the conclusions of this paper, it necessary to point out that the post-test pictures of CORA-17 bundle have been taken after the end of the quench phase, while in the simulated transient this phase is not taken into account. During the quenching, a great amount of steam is released within the bundle, thus more heat is generated through Zirconium-steam interaction, as already mentioned. Taking this in mind, the high under prediction of bundle melt in CORA-17 assumes less importance.

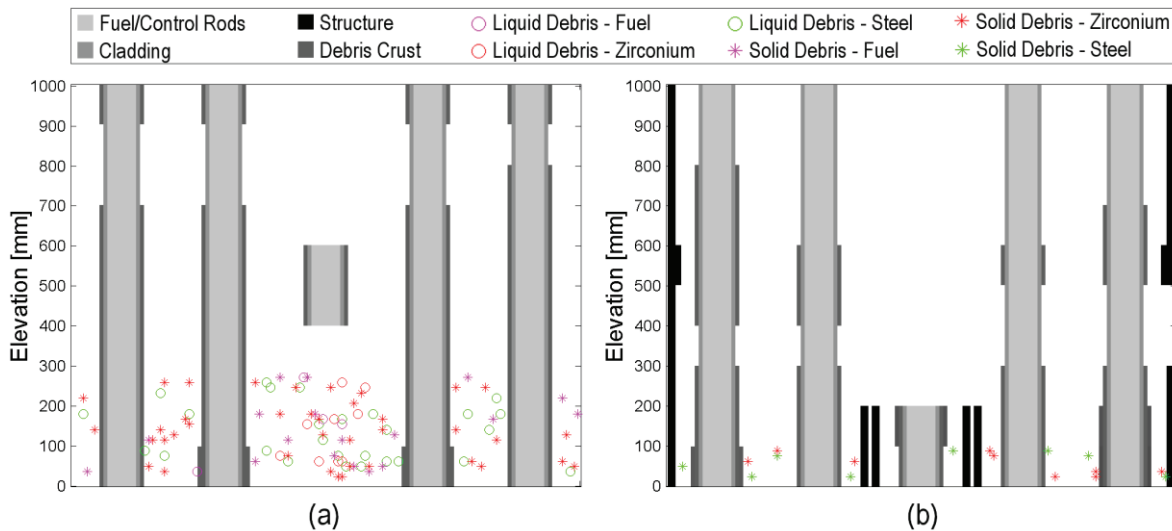


Figure 7. Side view on state of the bundle at the end of the simulated transients for CORA-17 (a) and CORA-18 (b).

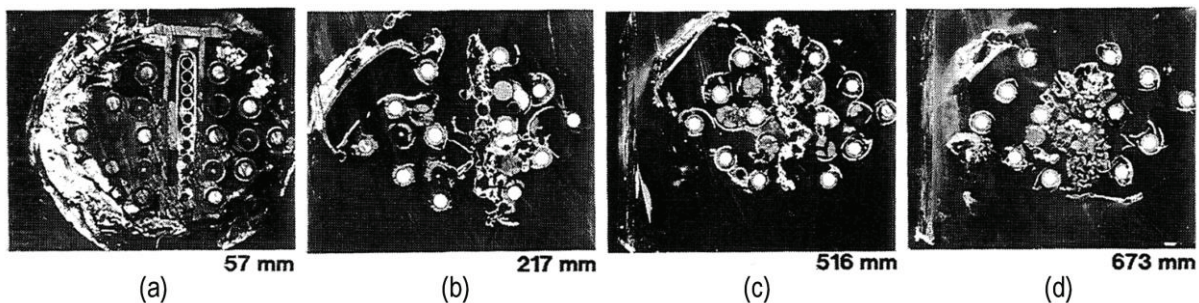


Figure 8. Horizontal cross sections of CORA-17 bundle at the end of the transient at different height: (a) 57 mm, (b) 217 mm, (c) 516 mm, (d) 673 mm [4].

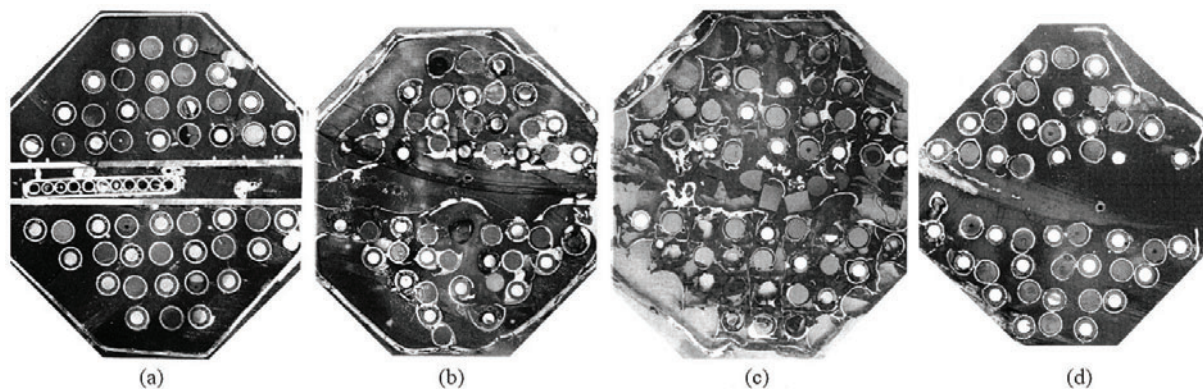


Figure 9. Horizontal cross sections of CORA-18 bundle at the end of the transient at different height: (a) 97 mm, (b) 413 mm, (c) 560 mm, (d) 702 mm [5].

5. CONCLUSIONS

The simulation results presented in this paper have demonstrated the capability of SAMPSON/MCRA to predict severe accidents with different levels of core melting. The early stages of the simulated experiments, i.e. when hydrogen generation is negligible, have been successfully predicted in both CORA experiments. Nevertheless in the later stages, the hydrogen generation is over predicted by the code in both simulated transients, especially in the CORA-17 one. As a consequence, also temperatures are over predicted in the later stage leading to a higher hydrogen generation rate (i.e. positive feedback). This is true also for CORA-18, although with less consequences. Although these consideration, the melting results are slightly under predicted in both tests, especially in the CORA-18 due to the absence of the quench phase in CORA-17 simulation.

Future developments will investigate the reason of the hydrogen over prediction. Moreover the dependence of emissivity ϵ from temperature and thickness of oxide layer on Zirconium structures and cladding will be modeled and included in the code. The modeling of the grid spacer should be further implemented and the quench phase of CORA-17 will be simulated. Moreover the refinement of the existing physical models represents a main task for the future.

REFERENCES

1. W. Hering, P. Hofmann, “*Material Interactions during Severe LWR Accidents*”. KfK 5125, Kernforschungszentrum Karlsruhe GmbH, Karlsruhe, Germany, 1994.
2. M. Steinbrück, “*Influence of boron carbide on core degradation during severe accidents in LWRs*”. Annals of Nuclear Energy, vol. 64, pp. 43-49, 2014.
3. S. Hagen, P. Hofmann, V. Noack, L. Sepold, G. Schanz, G. Schumacher, “*Comparison of the Quench Experiments CORA-12, CORA-13, CORA-17*”. FZKA 5679, Kernforschungszentrum Karlsruhe GmbH, Karlsruhe, Germany, 1996.
4. L. Sepold, S. Hagen, P. Hofmann, G. Schanz, “*Behavior of BWR-type Fuel Elements with B₄C/Steel Absorber Tested under Severe Fuel Damage Conditions in the CORA Facility*”. FZKA 7447, Kernforschungszentrum Karlsruhe GmbH, Karlsruhe, Germany, 2009.
5. S. Hagen, P. Hofmann, V. Noack, L. Sepold, G. Schanz, G. Schumacher, “*Large Bundle BWR Test CORA-18: Test Result*”. FZKA 6031, Kernforschungszentrum Karlsruhe GmbH, Karlsruhe, Germany, 1998.

6. A. Costa, M. Pellegrini, H. Mizouchi, H. Suzuki, M. Naitoh, H. Ninokata, M. E. Ricotti, “*Validation of the SAMPSON/MCRA code against CORA-18 experiment*”. Proceedings of ICONE 23, Chiba, Japan, 2015.
7. G. Schanz, B. Adroguer, A. Volchek, “*Advanced treatment of zircaloy cladding high-temperature oxidation in severe accident code calculations: Part I. Experimental database and basic modeling*”. Nuclear Engineering and Design, vol. 232, pp. 75-84, 2004.
8. P. Hofmann, M. Markiewicz, J. Spino, “*Reaction Behavior of B₄C Absorber material with Stainless Steel and Zircaloy in Severe LWR Accidents*”. KfK 4598, Kernforschungszentrum Karlsruhe GmbH, Karlsruhe, Germany, 1989.
9. P. Hofmann, M. Markiewicz, “*Chemical Interactions between as-received and pre-oxidized Zircaloy-4 and Stainless Steel at High Temperatures*”. KfK 5106, Kernforschungszentrum Karlsruhe GmbH, Karlsruhe, Germany, 1994.
10. T. Haste, M. Steinbrück, M. Barrachin, O. de Luze, M. Grosse, J. Stuckert, “*A comparison of core degradation phenomena in the CORA, QUENCH, Phébus SFD and Phébus FP experiments*”. Nuclear Engineering and Design, vol. 283, pp. 8-20, 2014.